ESTIMATIONS OF HALF-LIVES OF FAR-SUPERHEAVY NUCLEI WITH $Z \approx 154$–164

BY A. ŁUKASIAK AND A. SOBICZEWSKI

Institute for Nuclear Research, Warsaw*

(Received February 8, 1974)

The spontaneous fission and alpha-decay half-lives of doubly-even superheavy nuclei with $Z \approx 154$–164 are calculated microscopically. The beta stability is also investigated.

The longest total half-lives of the order of 10^5–10^7 years are obtained for nuclei in the neighbourhood of doubly magic nucleus $^{472}(164)$.

1. Introduction

Theoretical calculations of the lifetimes of superheavy nuclei close to the doubly-magic nucleus $^{298}(114)$ have shown (cf. e. g. Refs [1–6]) that the shell effects may result in very long, as for such nuclei, half-lives. The half-lives are of the order of 10^{10} years.

According to the extrapolated single-particle spectra of various realistic nuclear potentials, the nucleus $^{298}(114)$ is expected to be the closest doubly magic nucleus to the empirical region.

A natural question is whether one can expect heavier doubly magic nuclei with reasonably long lifetimes.

The calculations with spherical Nilsson potential [7–9] predict the number $Z = 164$ as a good candidate (large energy gap) for the proton closed shell. The shell is rather stable against changes of the potential parameters. However, the neutron energy gaps obtained in these calculations are small and rather sensitive to the potential parameters.

The calculations [10] with the Woods-Saxon potential support the number $Z = 164$ as a good candidate for the proton closed shell.

However, additionally, a subshell at $Z = 154$ and a whole region of a low level density in the proton spectrum at $Z = 154$–164 appear in these calculations. Also in distinction to the calculations with the Nilsson potential, these calculations lead to the strong and rather stable neutron shells. The shells appear at $N = 228$, 308 and 406. The shell at $N = 228$ is slightly weaker and less stable than these at $N = 308$ and 406.

The situation is illustrated in Fig. 1 taken from Ref. [10]. After the first superheavy island of increased stability **1**, concentrated around the nucleus $^{298}(114)$, which attracts

* Address: Instytut Badań Jądrowych, Hoża 69, 00-681 Warszawa, Poland.

now much of theoretical and experimental interests, there appear the islands **2–3** and **4**. The island **4** is connected with the large and stable neutron shell $N = 308$. The island **2–3** is connected with the smaller and less stable shell $N = 228$.

The crude estimations [10] of the alpha-decay and spontaneous fission lifetimes, T_α and T_{sf}, respectively, show that very short T_α are expected for region **2–3** due to the strong

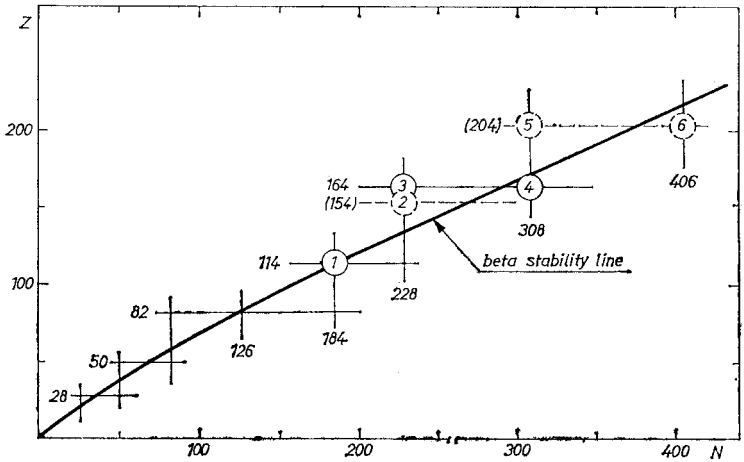

Fig. 1. Positions of the predicted doubly magic very heavy nuclei on the nuclear chart. The extrapolated empirical beta stability line is shown

neutron-deficiency of this region. However, rather long lifetimes, both T_α and T_{sf}, are expected in region **4**. Also in this region the beta-stable nuclei may appear in connection with the nearness of this region to the extrapolated empirical beta-stability line.

The purpose of the present investigation is to perform the microscopic calculations of the half-lives T_α and T_{sf}, and also the calculations of the positions of beta-stable nuclei in both regions **2–3** and **4**.

In Sect. 2 we describe the calculations, in Sect. 3 we present the results and in Sect. 4 we discuss them. Sect. 5 gives the conclusions.

Some of the results of the present research have been given in Ref. [11].

2. Description of the calculations

As mentioned in the Introduction, we aim at calculating the spontaneous fission and the alpha-decay half-lives of doubly even nuclei in their ground states and at finding the position of the beta-stability line in the regions **2–3** and **4**.

2.1. Method of the calculations

The spontaneous fission half-life T_{sf} is calculated according to the formula

$$T_{sf} = \frac{\ln 2}{n} \frac{1}{P}, \tag{1}$$

where n is the number of assaults of a nucleus on the fission barrier per unit time and P is the probability of penetration of the nucleus through the barrier for a given assault. The frequency of a vibration leading to fission (here beta-vibration) is usually taken for n.

In the one-dimensional case, considered here, the WKB approximation gives for the penetrability P through the barrier

$$P = \left\{1+\exp\left(2\int_{\varepsilon_1}^{\varepsilon_2}\sqrt{2\frac{B(\varepsilon)}{\hbar^2}[W(\varepsilon)-E]}\,d\varepsilon\right)\right\}^{-1}, \tag{2}$$

where ε is the deformation parameter, $W(\varepsilon)$ is the potential energy barrier and E is the energy of the nucleus in the fissionning state, as illustrated schematically in Fig. 2. The mass parameter $B(\varepsilon)$ describes the inertia of the nucleus with respect to the deformation ε.

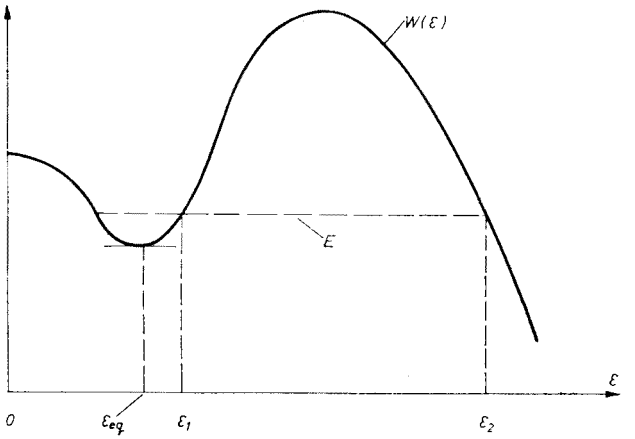

Fig. 2. Schematic fission barrier. For nuclei close to a doubly magic nucleus $\varepsilon_{eq} = 0$

To get the energy barrier, we calculate the binding energy of a nucleus as a function of deformation. We assume the energy to be composed of a smooth phenomenological part, described by the liquid drop model, and of the shell correction, i. e.

$$E(Z, N, \varepsilon) = E_{LD}(Z, N, \varepsilon)+\Delta E_{SHELL}(Z, N, \varepsilon). \tag{3}$$

The shell correction is calculated microscopically by the Strutinsky method [12]. It consists of the proton and the neutron contributions

$$\Delta E_{SHELL}(Z, N, \varepsilon) = \Delta E_{SHELL}(Z, \varepsilon)+\Delta E_{SHELL}(N, \varepsilon), \tag{4}$$

each of which, after inclusion of the residual pairing interaction by the BCS formalism, is of the form [3]

$$\Delta E_{SHELL}(X, \varepsilon) = \{\sum_{\nu} e_\nu 2v_\nu^2-\Delta^2/G-G(\sum_{\nu} v_\nu^4-\sum_{\nu}' 1)\}-\{E(g)+\langle E_{pair}\rangle\}, \tag{4a}$$

where X stands for Z (protons) or N (neutrons). In Eq. (4a) e_ν is the energy and v_ν^2 is the occupation factor of the single-particle state $|\nu\rangle$, G is the pairing force strength and 2Δ is the pairing energy gap. The term $G\sum'1$ is the diagonal pairing energy corresponding to the sharp Fermi surface.

The quantity $E(g)$ represents the sum of the energies of the single-particle levels when these levels are smeared out to give a continuous density $g(e)$. The corresponding formula is

$$E(g) = \int_{-\infty}^{e_F} 2eg(e)de, \tag{5}$$

where the Fermi energy e_F is given by

$$X \equiv Z(\text{or } N) = \int_{-\infty}^{e_F} 2g(e)de. \tag{5a}$$

The level density function $g(e)$ smeared out with the help of the Gauss function is

$$g(e) = \frac{1}{\gamma\sqrt{\pi}} \sum_\nu f_{\text{corr}}(u_\nu) e^{-u^2\nu}, \tag{6}$$

where $u_\nu = (e-e_\nu)/\gamma$. The role of the function $f_{\text{corr}}(u_\nu)$ is to correct, reconstruct the long--range (the range of the order of the Fermi energy e_F) behaviour of the level density distorted by smearing out of the short-range (of the order of the shell spacing $\hbar\omega_0$) fluctuations of this density. We have taken here $\gamma = 1.0\ \hbar\omega_0$ for the smearing parameter and the sixth-order polynomial for the correction function $f_{\text{corr}}(u_\nu)$. For the average pairing energy $\langle E_{\text{pair}}\rangle$, here, we take after Ref. [3], the value -2.3 MeV.

The mass parameter B is calculated microscopically in the adiabatic approximation. The corresponding formula is [13]

$$\frac{1}{\hbar^2} B = \frac{2\Sigma_3}{(2\Sigma_1)^2} \left(\frac{\partial Q}{\partial \varepsilon}\right)^2, \tag{7}$$

where

$$\Sigma_n = \sum_{\mu,\nu} \frac{\langle\mu|\hat{q}|\nu\rangle^2 (u_\mu v_\nu + u_\nu v_\mu)^2}{(E_\mu + E_\nu)^n} + \Delta\Sigma_n,$$

with $n = 1$ or 3. Here $\hat{q}$ is the single-particle quadrupole moment operator, u_ν and v_ν are the BCS variational parameters and E_ν is the quasiparticle energy corresponding to the single-particle state $|\nu\rangle$. The quantity Q is the total (mass) quadrupole moment of a nucleus and $\Delta\Sigma_n$ is the contribution to Σ_n coming from the coupling of the quadrupole collective motion to the pairing vibrations as discussed in Ref. [13].

In Sect. 3 we compare the microscopic values of B obtained from Eq. (7) with the phenomenological ones obtained from the spontaneous fission lifetimes of heavy nuclei [1].

To estimate the alpha-decay half-lives T_α, we use two alternative phenomenological formulae. One given by Taagepera and Nurmia [14]

$$\log T_\alpha(y) = 1.61\left[\frac{Z-2}{\sqrt{Q_\alpha}} - (Z-2)^{2/3}\right] - 28.9, \tag{8}$$

and the other by Viola and Seaborg [15]

$$\log T_\alpha(\text{sec}) = \frac{A_Z}{\sqrt{Q_\alpha}} + B_Z, \tag{9}$$

where

$$A_Z = 2.11329\ Z - 48.9879$$

$$B_Z = -0.39004\ Z - 16.9543.$$

In both formulae (8) and (9) Z is the atomic number of a parent nucleus and Q_α is the alpha-decay energy in MeV. To obtain Q_α, we calculate the difference between the ground-state energies of parent and daughter nuclei, both obtained from Eq. (3), and diminish it by the empirical alpha particle energy.

To find the position of the beta-stability line, we need, besides the ground-state energy of a doubly even nucleus, also the energy of doubly odd nucleus. We find the last one in two variants. One when the energy of an odd number of protons or neutrons is calculated with blocking of the single-particle state occupied by the odd particle, and the other without blocking. In the variant with blocking, we get a lower number of beta stable nuclei due to a smaller pairing energy gap 2Δ obtained in this case. The blocking of one single-particle state lowers the efficiency of the pairing interaction, and thus it lowers the gap 2Δ.

2.2. Details of the calculations

To describe the dependence of both the energy and the mass parameter of a nucleus on deformation, we use the Nilsson potential. We require, however, of the potential to reproduce the Woods-Saxon potential spectra at zero deformation. This is because the Woods-Saxon potential appears to be relatively reliable for extrapolations of the spectra in the mass number, as discussed in Ref. [10].

In other words, we adopt here the spectra of the spherical Woods-Saxon potential obtained [10] for the regions **2–3** and **4**, and use the simple Nilsson potential for description of the deformation dependence of these spectra. This procedure was used in the earlier paper [5] for the calculation of life-times of nuclei in the region **1**, i. e. in the region of $Z \approx 114$.

Fig. 3 shows two variants of the Woods-Saxon spectra for protons. None of them is a spectrum of a definite nucleus with specified Z and A, but each is rather a "universal" spectrum of beta-stable nuclei, the spectrum which only locally corresponds to a definite nucleus.

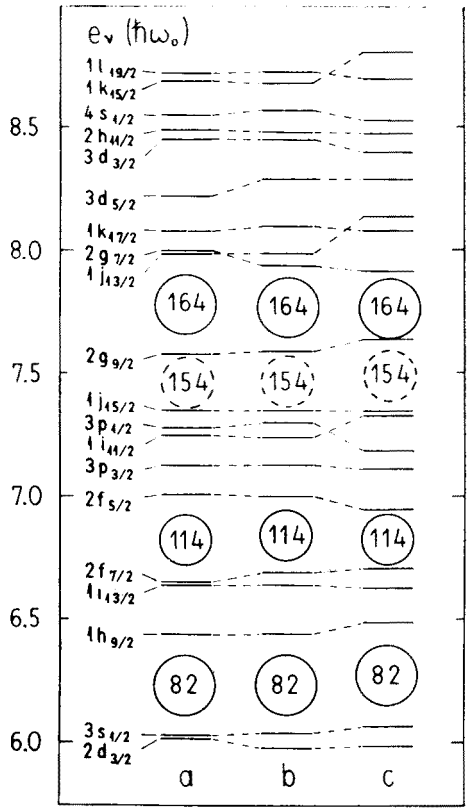

Fig. 3

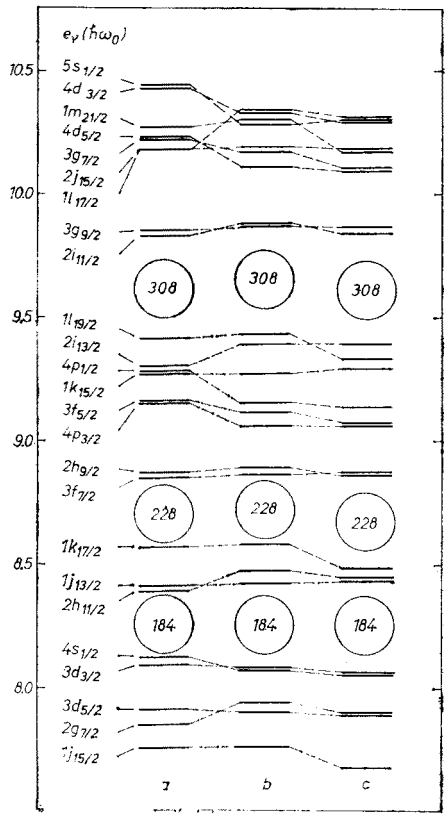

Fig. 4

Fig. 3. Single-particle schemes for protons in a spherical nucleus: a) Nilsson scheme used in the present paper b) Woods-Saxon scheme based on the Blomqvist-Wahlborn parameters c) Woods-Saxon scheme based on the Rost parameters

Fig. 4. Same as Fig. 3 for neutrons

The spectra are obtained in the following way. For given Z, the mass number A is found from the empirical formula [16] for the beta-stability line

$$N-Z=\frac{0.4A^2}{A+200}. \tag{10}$$

Then, with the potential parameters appropriate to those Z and A, few energy levels close to the Fermi level are found. Changing Z by few units, the next few levels are found and so on.

The "universal" spectrum obtained that way is locally good for the appropriate Z. In particular, it reproduces all empirical magic numbers, of which only $Z = 82$ is shown in the figure.

The corresponding spectra for neutrons are given in Fig. 4.

The spectra 3b and 4b correspond to the variant (*i*) of the potential parameters discussed in Ref. [10], i. e. to the parameters

$$r_0 = 1.27 \text{ fm}, \quad a_0 = 0.67 \text{ fm}, \quad \lambda = 32.0,$$

and

$$V_0^{p(n)} = 51 \left(1 \pm 0.67 \frac{N-Z}{A}\right) \text{MeV}, \tag{11}$$

where $R = r_0 A^{1/3}$ is the radius, a_0 the diffuseness, λ the spin-orbit coupling strength and V_0 the depth of the potential. The values of r_0, a_0 and λ are kept constant as functions of A, while the dependence of V_0 on A and Z, related by Eq. (10), is shown explicitly in Eq. (11). This variant of parameters is related to the analysis by Blomqvist and Wahlborn [17] for the Pb region (cf. also Ref. [18]).

The spectra 3c and 4c correspond to the variant (*ii*) of the parameters discussed in Ref. [10], and are related to the analysis by Rost. [19]. Here, the geometrical parameters r_0 and a_0, as well as the parameter λ, are again assumed to be constant with A, while the depth V_0 is

$$V_0^{p(n)} = 49.6 \left(1 \pm 0.86 \frac{N-Z}{A}\right) \text{MeV}. \tag{12}$$

The spectra 3a and 4a are those of the spherical Nilsson potential with the parameters κ, μ and $\hbar\omega_0$ fitted to the Woods-Saxon spectra 3b and 4b. The values of κ and μ, each being a function of the oscillator shell number N, are given in Table I. They are changed with respect to those used in Ref. [5] for the calculations of the lifetimes of superheavy nuclei in the region **1**. The change comes mainly from the fact that here the

TABLE I

The Nilsson scheme parameters κ and μ, used in the present calculation, versus shell number N

N	κ_p	κ_n	μ_p	μ_n
0	—	—	0	0
1	0.150	0.143	0	0
2	0.098	0.091	0.27	0.05
3	0.078	0.078	0.40	0.22
4	0.071	0.064	0.53	0.35
5	0.052	0.051	0.72	0.54
6	0.047	0.038	0.83	0.61
7	0.043	0.043	0.94	0.48
8	0.036	0.041	1.12	0.52
9	0.033	0.040	1.26	0.50
10	0.032	0.037	1.28	0.52
11	0.029	0.044	1.40	0.48
12	0.029	0.041	1.40	0.51
13	0.029	0.041	1.40	0.51
14	0.029	0.041	1.40	0.51

oscilator strength $\hbar\omega_0$ is also fitted to the Woods-Saxon spectra, as described below, while in Ref. [5] it was kept according to Eq. (13'). This allowed us to improve the fit. As κ and μ of Table I correspond to the "universal" spectrum they may be also used for other regions of nuclei than those analysed here.

The oscillator strength $\hbar\omega_0$ multiplied by $A^{1/3}$ reveals to be also a function of N (or A), similarly as κ and μ are. It is obtained that for protons

$$A^{1/3}\times\hbar\omega_0^p \approx 47.5 \text{ MeV} \tag{13a}$$

for both **2–3** and **4** while for neutrons

$$A^{1/3}\times\hbar\omega_0^n \approx \begin{cases} 45.4 \text{ MeV} & \text{for } \mathbf{2-3}, \\ 43.9 \text{ MeV} & \text{for } \mathbf{4}. \end{cases} \tag{13b}$$

Thus, for neutrons they are about the same and for protons they are larger than the values taken usually [3]

$$A^{1/3}\times\hbar\omega_0^{p(n)} = 41\left(1\mp\frac{1}{3}\frac{N-Z}{A}\right)\text{MeV}. \tag{13'}$$

All the results given in the present paper are obtained with the described "universal" Nilsson scheme fitted to the Woods-Saxon spectra 3b and 4b (Blomqvist-Wahlborn variant) at zero deformation. The effect of using the scheme fitted to 3c and 4c levels (Rost variant) instead of 3b and 4b is discussed in Sect. 4.

The pairing force strength is taken according to Ref. [3], i. e.

$$A\times G_{p(n)} = 19.2\pm 7.4\frac{N-Z}{A}\text{ MeV}, \tag{14}$$

with $2\sqrt{15\,Z(N)}$ levels nearest to the Fermi level, accounted when solving the pairing equations. As discussed in Sect. 4, also for so heavy nuclei as those in the **2–3** and **4** regions

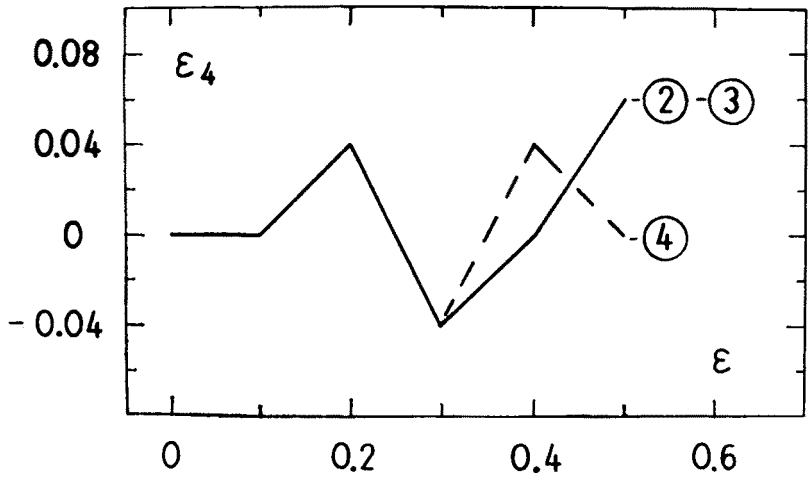

Fig. 5. The average minimum potential energy paths for regions 2–3 and 4

the strength (14) leads to Δ not far, on the average, from the extrapolated empirical values $\Delta \approx 12A^{-1/2}$ MeV, especially for neutrons.

Concerning the dependence of the strength G on deformation, we assume G to be proportional to the surface area of the nucleus, $G \propto S$.

The potential energy of a nucleus is calculated as a function of the quadrupole and hexadecapole deformations, ε and ε_4, respectively. We assume a nucleus to undergo fission along the static path, i. e. along the path of the minimal potential energy. The average path found for nuclei in the region **2–3**, as well as the average path found for the region **4**, are given in Fig. 5. All the results of T_{sf} are obtained with the use of these paths, the appropriate path for each region.

The liquid drop model parameters, needed in Eq. (3), are taken from the Lysekil paper by Myers and Swiatecki [20].

In the calculation of the fission probability P, Eq. (2), we assume, similarly as in papers [1, 3, 5, 6], that the height of the barrier is lowered by the zero point vibration energy $E - W(\varepsilon_{eq}) = \frac{1}{2}\hbar\omega_{vib} = 0.5$ MeV. The number of assaults on the barrier $n = 10^{20.38}$ sec^{-1} corresponding to $\hbar\omega_{vib} = 1$ MeV is taken.

3. *Results*

To see how quickly the shell correction ΔE_{SHELL} decreases when we go with the neutron or proton numbers off the magic values, we plot the contour maps of ΔE_{SHELL}. The maps give an idea of the size and of the shape of each island of the increased fission stability. They also give an idea of how large is the shell correction contribution to the alpha decay energy.

Fig. 6 presents such map for region **2–3**. It can be seen that the largest, in absolute value, shell correction is obtained for the nucleus $^{392}(164)$, i. e. for the nucleus with $Z = 164$

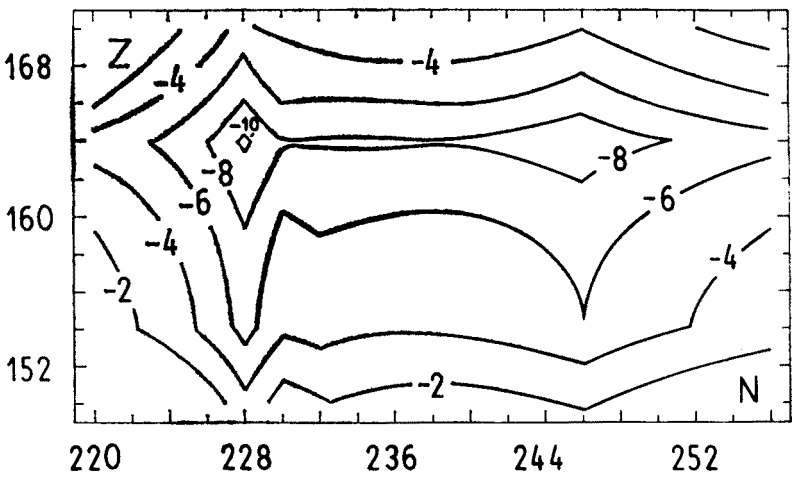

Fig. 6. Contour map of the shell correction ΔE_{SHELL} in MeV for region 2–3. The correction is calculated for the spherical shape of nuclei, using spectra (b) of Figs 3 and 4

and $N = 228$. The value of the correction is about 10 MeV, i. e. only slightly smaller than the value obtained [3] for ^{208}Pb (about 12 MeV). It can also be seen that the large correction obtained for the nuclei with the closed shell at $N = 228$ shows a tendency to extend to heavier nuclei, up to these with $N = 246$. This is due to the presence of a rather strong subshell at $N = 246$. The shell correction for the nucleus $^{410}(164)$ is around 9 MeV.

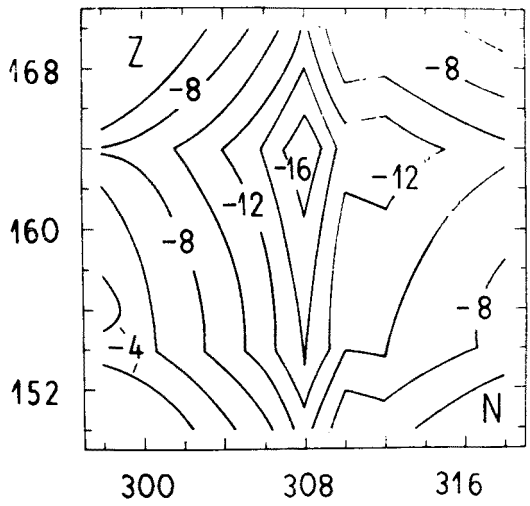

Fig. 7. Same as Fig. 6 for region **4**

The respective contour map for region **4** is presented in Fig. 7. Here, the largest value of ΔE_{SHELL} is especially high, around 18 MeV. It comes mainly from the very strong neutron shell at $N = 308$.

Both figures 6 and 7 are obtained with the single-particle levels of the spherical Woods-Saxon potential, Figs 3b and 4b.

Examples of the fission barriers are given in Fig. 8 for few isotones with $N = 228$ and in Fig. 9 for few isotopes with $Z = 164$. The barriers are calculated along the minimum potential energy paths of Fig. 5. The contribution of the liquid drop energy to each barrier is shown. It is seen that the barriers appear only because of the shell effect. On account of a large value of the fissility parameter (owing mainly to large Z), the contribution of the liquid drop to the barriers is negative and quite strong. Due to this the barriers are thin. They are about two times thinner than the barriers [1, 3, 5] in region **1**.

Fig. 10 illustrates the dependence of the microscopic mass parameter B^{micr} on the deformation for three isotopes with $Z = 154$. We take the same deformation paths of Fig. 5 as for the calculation of the potential barriers. The phenomenological values $B^{\text{phen}} = 0.054\ A^{5/3}\ \hbar^2\ \text{MeV}^{-1}$ obtained [1] from the spontaneous fission half-lives of actinides are shown for comparison. It is seen that B^{micr}, averaged in deformation, are larger than B^{phen}.

The spontaneous fission half-lives T_{sf} for region **2–3** are presented in Fig. 11. They are calculated with B^{micr}. The shapes of the lines of constant T_{sf} are rather similar to the shapes of the corresponding lines of constant ΔE_{SHELL} of Fig. 6. It is because the last ones

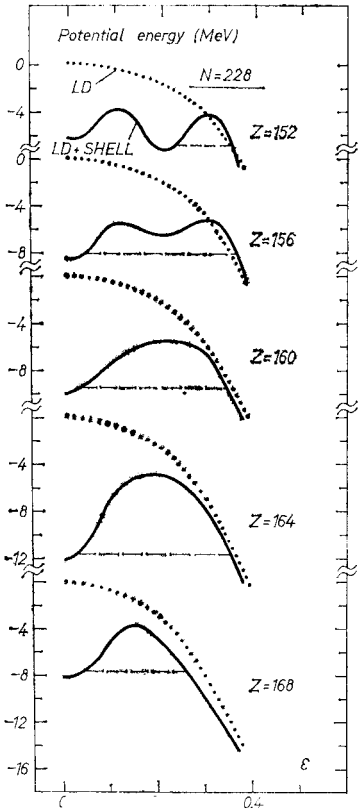

Fig. 8

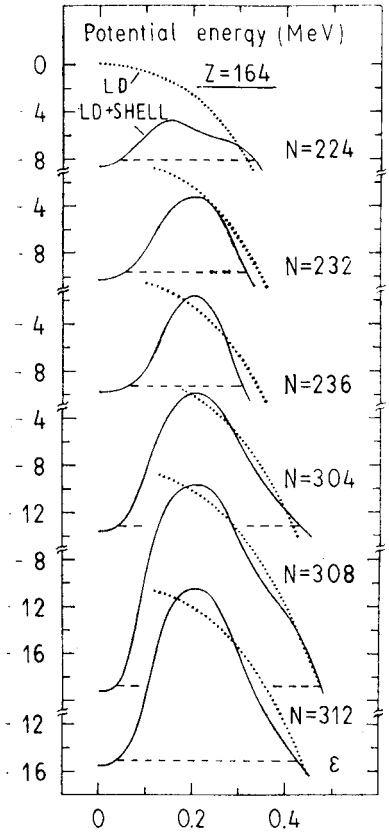

Fig. 9

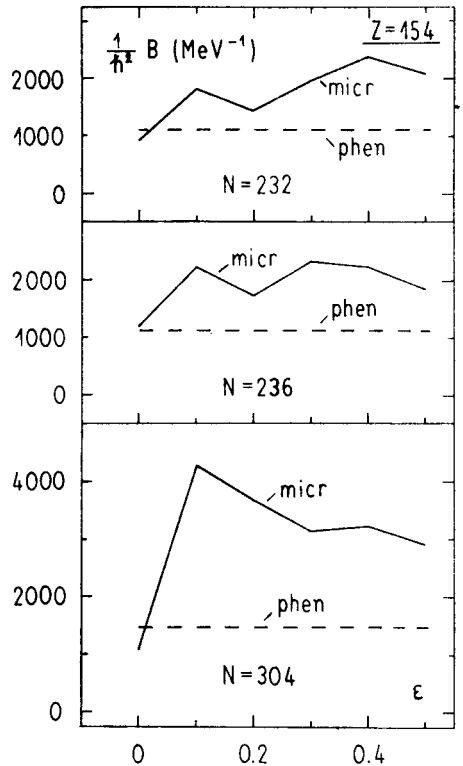

Fig. 10

Fig. 8. Fission barriers for few isotones with $N = 228$. The contribution of the liquid drop energy to each barrier is shown. The dashed straight line cutting each barrier corresponds to the zero-point energy equal to 0.5 MeV·

Fig. 9. Same as Fig. 8 for few isotopes with $Z = 164$

Fig. 10. Mass parameter B calculated microscopically as a function of deformation for three isotopes with $Z = 154$

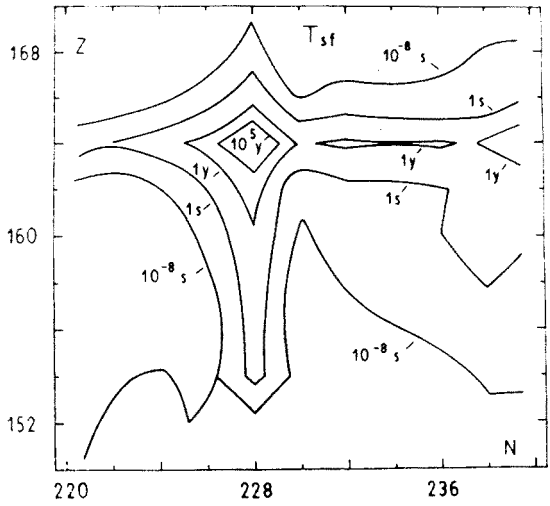

Fig. 11. Map of the spontaneous fission half-lives T_{sf} for region **2–3**

correspond, roughly, to the lines of constant height of the barriers. It is seen that the largest value of T_{sf} in region **2–3** exceeds 10^5 y.

The half-lives T_{sf} for region **4** are given in Fig. 12. They are even longer than these for region **2–3**. This is because of larger values of both barriers and mass parameters.

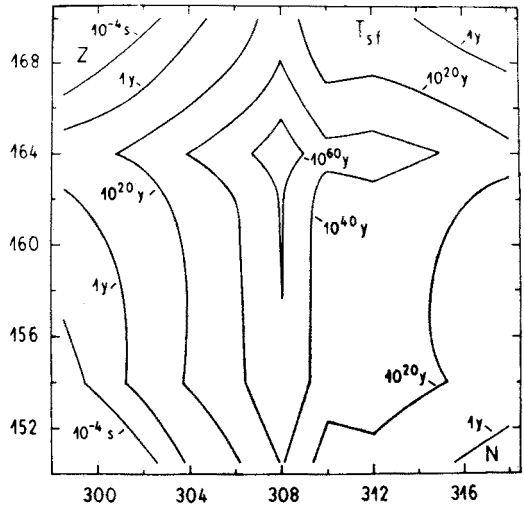

Fig. 12. Same as Fig. 11 for region **4**

Before considering the alpha-decay half-lives T_α, let us look at the alpha-decay energies Q_α.

They are given in Fig. 13 for region **2–3**. It is seen that the lines of constant value of Q_α have rather complicated shapes as compared to regular shapes obtained from the pure

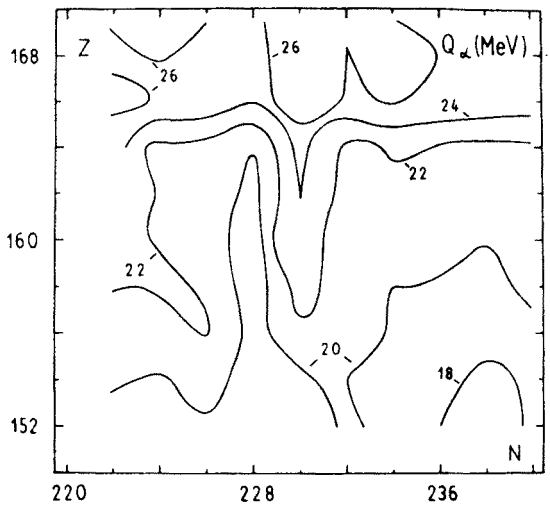

Fig. 13. Map of the alpha-decay energies Q_α for region 2–3. The numbers on the contour lines give the values of Q_α in MeV

liquid drop. These "complications" come from the shell correction ΔE_{SHELL} which manifests in Q_α through two effects. One is the direct change of Q_α by ΔE_{SHELL} when the alpha transition occurs between spherical nuclei. The other is the effect of the deformation energy on Q_α when the transition between nuclei with different deformations takes place.

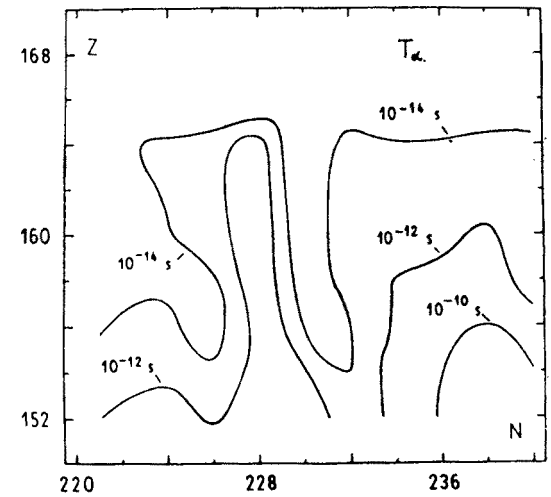

Fig. 14. Map of the alpha-decay half-lives T_α for region 2–3

For given Z and N of a parent nucleus, the first effect increases Q_α when the decay proceeds towards the magic nucleus and decreases it when the decay proceeds outwards the magic nucleus. The second effect results in just the opposite, but it manifests mostly

in the transitional region between spherical and deformed nuclei, i. e. around 6–10 mass units apart from a magic number, while the first effect is strongest in the closest neighbourhood of a magic number, i. e. for spherical nuclei.

Both effects can be easily seen in Fig. 13.

The alpha-decay half-lives T_α are given in Fig. 14. They are calculated from formula (8). Formula (9) usually gives T_α slightly shorter.

The lines of constant T_α are similar in shape to the lines of constant Q_α, Fig. 13. The lines corresponding to T_α, smaller than 10^{-14} s, are not shown in the figure.

A comparison between Figs 14 and 11 shows that T_α are shorter than T_{sf} in almost all region **2–3**. Thus, the longest half-lives, with respect to both alpha and fission decays, occur for nuclei for which T_α is the longest. These longest half-lives appear for nuclei around $^{392}(154)$ and around $^{386}(158)$ and are of the order of $10^{-9}-10^{-10}$ s.

No beta-stable doubly-even nucleus is found in all region **2–3** presented in Figs 14 or 11.

The appearance of very short T_α in region **2–3** is due to the large value of Z and additionally to strong neutron-deficiency of nuclides in this region. The alpha-decay energy Q_α, described in gross by the liquid drop model, is very large for such nuclides,

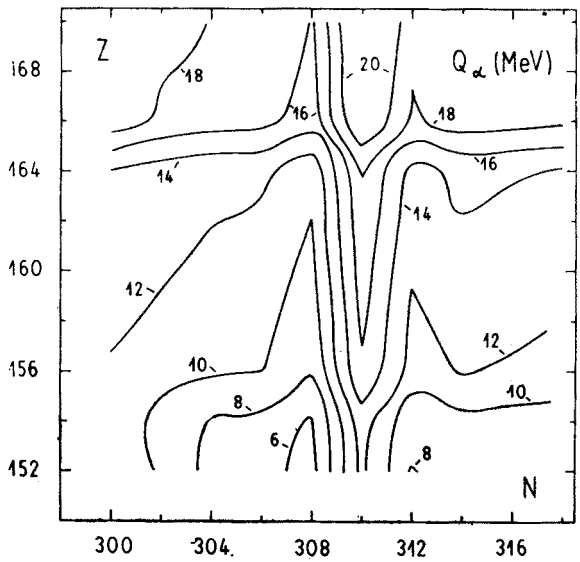

Fig. 15. Map of the alpha-decay energies Q_α for region **4**

and even a remarkable shell correction cannot change it much. As can be seen in Fig. 6, this shell correction to Q_α does not exceed 3.5 MeV, while the liquid-drop part of Q_α is about 20 MeV.

For example, the decomposition of Q_α to liquid drop and shell correction parts for $^{392}(164)$ is $Q_\alpha = Q_\alpha^{LD} + Q_\alpha^{SHELL} = 23.6 - 3.5 = 20.1$ MeV. This Q_α results in $T_\alpha = 10^{-11}$ s. The corresponding decomposition of Q_α for the nucleus $^{298}(114)$ from region **1** is $Q_\alpha =$

$= 9.4-2.7 = 6.7$ MeV. This Q_α results in $T_\alpha \approx 10^4$y. Thus, although the shell correction in region **2–3** is slightly larger than in region **1**, it cannot compensate the strong increase in the liquid drop part of Q_α when going from region **1** to **2–3**.

The alpha-decay energies Q_α for region **4** are given in Fig. 15 and the lifetimes T_α in Fig. 16. The lifetimes T_α are calculated from formula (8).

It is seen that T_α here are much longer than for region **2–3**. It is because the nuclei in region **4**, having the same number of protons Z, have about 80 neutrons more than the nuclei in region **2–3**.

As a result, taking also into account the larger T_{sf}, the total half-lives with respect to both alpha-decay and fission are much longer than in **2–3**. The longest lifetimes are obtained for nuclei around $^{460}(152)$ and are of the order of 10^{30}–10^{40} y.

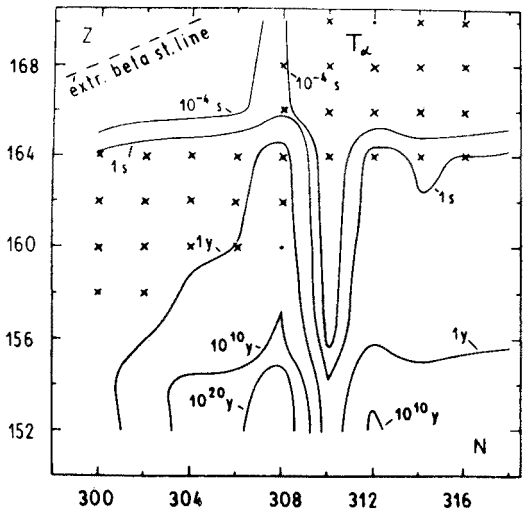

Fig. 16. Map of the alpha-decay half-lives T_α for region **4**. The beta-stable even-even nuclei are shown (solid points). The crossed solid points denote the beta-stable nuclides obtained when the blocking procedure is used. The position of the extrapolated empirical beta-stability line is indicated (dashed line)

However, if one takes into account only beta-stable nuclides, the longest half-life is obtained for the nucleus $^{470}(162)$ and is of the order of 10^5 y, when the variant of calculation with blocking (cf. Sect. 2) is taken, and for the nucleus $^{468}(160)$, and is of the order of 10^7 y in the variant without blocking.

The positions of the beta-stable even-even nuclei are indicated in Fig. 16 by solid points. The crossed solid points denote the nuclides which are beta-stable in both variants of the calculation. Each beta-stable nucleus in variant with blocking (smaller pairing energy gap 2Δ) is also beta-stable in variant without blocking but not vice versa. The number of beta-stable nuclides in variant without blocking is slightly larger.

As can be seen in Fig. 16, all beta-stable nuclei obtained microscopically are situated below the extrapolated empirical beta-stability line [16] given by Eq. (10), and indicated in Fig. 16 by dashed line.

4. Discussion

Let us first relate our results to the previous estimates [8, 9]. Doing this we should remember that we base on other single-particle spectra than those used in Refs [8, 9]. The spectra are especially different for neutrons. Due to this the different positions of the increased stability islands are obtained in our research and in the previous ones [8, 9]. Additionally, owing to stronger neutron shells in our spectra we generally get longer lifetimes. In fact, the longest lifetimes obtained in Ref. [9] (only in this reference both T_α and T_{sf} and also the positions of beta-stable nuclei are investigated microscopically) are about 10^{-2}–10^{-1} s and appear in the neighbourhood of the nucleus $^{466}(164)$. In our calculations, the longest lifetimes are about 10^5–10^7 y and occur nearby the nucleus $^{472}(164)$.

Now, let us discuss few factors influencing the lifetimes.

4.1. Pairing force strength

It is found (cf. e. g. Ref. [18], p. 170) that the empirical pairing energy gap 2Δ is well reproduced, on the average, by the formula

$$\Delta = 12A^{-1/2}\ \text{MeV}. \tag{15}$$

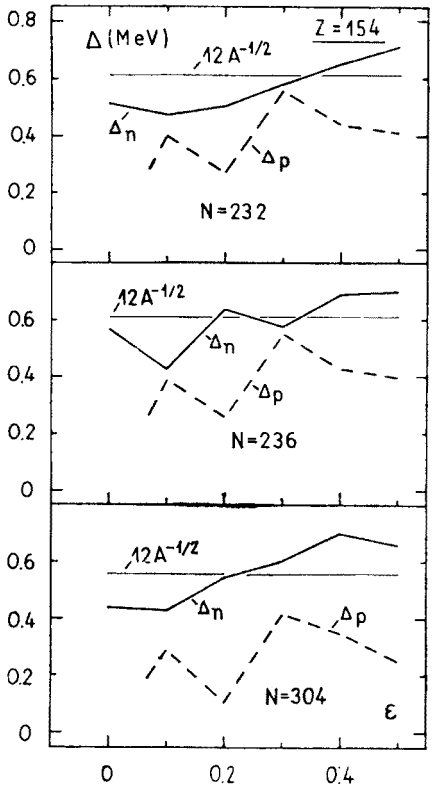

Fig. 17. Neutron and proton pairing energy gap parameters Δ_n and Δ_p, respectively, calculated as functions of the deformation, for three isotopes of $Z = 154$. The extrapolated empirical average values $\Delta = 12\ A^{1/2}$ MeV are shown for comparison

The pairing interaction strength G and the number of levels we use in the calculations (cf. Sect. 2) allow us to reproduce quite well the empirical Δ of Eq. (15) in the rare-earth and actinide regions [3]. It is interesting to see how well are the Δ of Eq. (15) reproduced by our calculations in the regions of very heavy nuclei we investigate here.

Fig. 17 shows Δ_n and Δ_p calculated as functions of deformation for three isotopes of $Z = 154$, the same isotopes as chosen in Fig. 10 for illustration of the deformation dependence of the mass parameter B. We can see that the theoretical values of Δ_n are quite close, on the average, to the values given by Eq. (15). The theoretical values of Δ_p, however, are smaller than the values (15).

Concerning the dependence of the pairing strength on deformation, the two cases: one of G constant with deformation (G = const.), and the other of G proportional to the area of the nuclear surface ($G \propto S$) are usually used. We use here only the second case, $G \propto S$, leading to smaller barriers and mass parameters, and thus to smaller lifetimes T_{sf}, as discussed in Refs [3, 5]. This choice corresponds to our intention of estimating rather ower than upper limits of the lifetimes.

4.2. Single-particle level scheme

As mentioned in Sect. 2, all the results for T_{sf} and T_α presented in the paper are obtained with the Nilsson scheme fitted, at zero deformation, to variant b (Figs 3 and 4) of the Woods-Saxon levels.

Let us take a quick look at possible effects of using the scheme fitted to variant c of the Woods-Saxon levels, instead of b. This variant corresponds to more recent than b analysis [19] of the empirical data.

We can see in Figs 3 and 4 that the energy gaps in variant c are: at $Z = 154$ slightly larger, at $N = 228$ considerably larger, at $N = 308$ about the same, and at $Z = 164$ slightly smaller than the respective gaps in b. We can expect then that the lifetimes for region **2–3**, and in particular for region **2**, may be considerably longer. Especially, if the increase in both shells at $Z = 154$ and $N = 228$ is strong enough to make the nucleus $^{378}(152)$, which is the daughter nucleus of $^{382}(154)$, spherical. In variant b this daughter nucleus is deformed while the parent nucleus is spherical. This fact results in a rather small alpha lifetime $T_\alpha \approx 10^{-11}$ s of the parent nucleus. In the case when the daughter nucleus is also spherical, the decay energy Q_α is decreased by about 3.5 MeV and T_α is respectively increased by about 6 orders.

Concerning region **4**, the use of variant c of the scheme, instead of b, may result in some, rather not large, decrease in the lifetimes T_α and T_{sf}.

4.3. Use of B^{phen} instead of B^{micr} in the calculations of T_{sf}

We have seen in Fig. 10 that the microscopic values of the mass parameter B^{micr} are in both regions **2–3** and **4** larger, on the average, than the extrapolated phenomenological values $B^{phen} = 0.054\ \hbar^2 A^{5/3}$ MeV^{-1}. For actinides B^{micr} are rather close or even slightly smaller than B^{phen}. This is illustrated in Fig. 18 for ^{238}U.

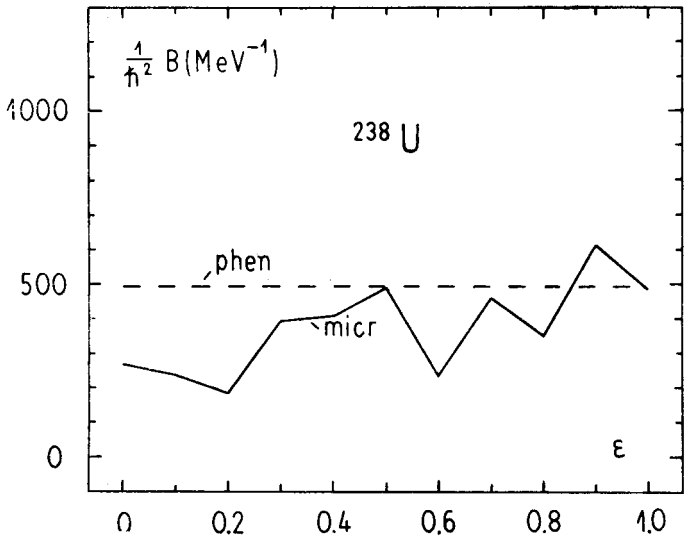

Fig. 18. Mass parameter B calculated microscopically as function of the deformation for ^{238}U. The phenomenological value is shown for comparison

Then it looks that B^{micr} increase more quickly with A than B^{phen} for which the hydrodynamical dependence on A is assumed.

The use of B^{phen} instead of B^{micr} in the calculations leads then to smaller values of T_{sf} in both regions **2–3** and **4**. However, the longest lifetimes among the beta-stable nuclei in region **4** are not decreased by this change, as T_α is decisive for these nuclei. Similarly, the longest lifetimes in region **2–3** remain almost unaffected by this change.

5. Conclusions

Summarizing the present research we can state the following:

1) Ater region **1** situated around the nucleus ^{298}(114) and closest to the empirical region, the next two, rather far, regions of an increased stability **2–3** and **4** are obtained.

2) Nuclei of region **2–3** are strongly neutron-deficient. They are far off the beta-stability line. Due to the large Z and the strong neutron-deficiency, their alpha lifetimes are short. They are of the order of only 10^{-9}–10^{-10} s or in the case of more favourable single-particle scheme (cf. discussion in Sect. 4.2) about 6 orders longer.

Although one can find out [10] reactions between known heavy nuclei in which, in principle, they could be produced, the real chance of such production may be very small. The effect of the centrifugal barrier may reduce the cross section of the reaction practically to zero [21].

3) Nuclei of region **4** have long lifetimes, of the order of 10^5–10^7 years, which is quite impressive if one remembers how large Z they have. However, because of the large number of neutrons they have, it is difficult to imagine a way of getting them in the earth conditions. Their creation would need rather special astrophysical conditions.

4) At last, one should stress the rough and estimative character of the results due to the very far extrapolations. Still, when having a choice in all uncertainties in getting them, we tried to keep close to lower rather than upper limit of the lifetimes.

The authors would like to thank Professor Z. Szymański and Dr. K. Pomorski for helpful discussions.

REFERENCES

[1] S. G. Nilsson, J. R. Nix, A. Sobiczewski, Z. Szymański, S. Wycech, C. Gustafson, P. Möller, *Nucl. Phys.* **A115**, 545 (1968).
[2] S. G. Nilsson, S. G. Thompson, C. F. Tsang, *Phys. Lett.* **28B**, 458 (1969).
[3] S. G. Nilsson, C. F. Tsang, A. Sobiczewski, Z. Szymański, S. Wycech, C. Gustafson, I. L. Lamm, P. Möller, B. Nilsson, *Nucl. Phys.* **A131**, 1 (1969).
[4] Yu. A. Muzychka, *Yad. Fiz.* **10**, 113 (1969).
[5] A. Łukasiak, A. Sobiczewski, W. Stępień-Rudźka, *Acta Phys. Pol.* **B2**, 535 (1971).
[6] E. O. Fiset, J. R. Nix, *Nucl. Phys.* **A193**, 647 (1972).
[7] C. Gustafson, I. L. Lamm, B. Nilsson, S. G. Nilsson, *Ark. Fys.* **36**, 613 (1967).
[8] J. Grumann, U. Mosel, B. Fink, W. Greiner, *Z. Phys.* **228**, 371 (1969); U. Mosel, W. Greiner, *Z. Phys.* **222**, 261 (1969).
[9] R. Bengtsson, *Proc. of the Int. Conf. on the Properties of Nuclei Far from the Region of Beta-Stability*, Leysin 1970, CERN 70-30, Geneva 1970, p. 646.
[10] A. Sobiczewski, T. Krogulski, J. Błocki, Z. Szymański, *Nucl. Phys.* **A168**, 519 (1971).
[11] A. Łukasiak, A. Sobiczewski, *Proc. Int. Conf. on Nuclear Physics*, Munich, 1973, ed. by J. de Boer and H. J. Mang, North-Holland/American Elsevier, 1973, vol. 1, p. 600.
[12] V. M. Strutinsky, *Nucl. Phys.* **A95**, 420 (1967); **A122**, 1 (1968).
[13] A. Sobiczewski, Z. Szymański, S. Wycech, S. G. Nilsson, J. R. Nix, C. F. Tsang, C. Gustafson, P. Möller, B. Nilsson, *Nucl. Phys.* **A131**, 67 (1969).
[14] R. Taagepera, M. Nurmia, *Ann. Acad. Sci. Fenn. Ser. A.* VI, No. 78, 1 (1961).
[15] V. E. Viola, Jr. G. T. Seaborg, *J. Inorg. Nucl. Chem.* **28**, 741 (1966).
[16] A. E. S. Green, *Nuclear Physics*, McGraw-Hill Book Co., New York 1955, p. 250.
[17] J. Blomqvist, S. Wahlborn, *Ark. Fys.* **16**, 545 (1960).
[18] A. Bohr, B. R. Mottelson, *Nuclear Structure*, Benjamin, New York 1969, vol. 1, p. 239.
[19] E. Rost, *Phys. Lett.* **26B**, 184 (1968).
[20] W. D. Myers, W. J. Swiatecki, *Ark. Fys.* **36**, 343 (1967).
[21] J. Wilczyński, *Proc. Third IAEA Symp. on the Physics and Chemistry of Fission*, Rochester 1973, IAEA, Vienna 1974, to be published; *Nucl. Phys.* **A216**, 386 (1973).